Synthesis, reactivity, structure and electronic properties of $[N(CH_3)_4]C_{60}\cdot 1.5thf$: fullerides with simple hexagonal packing

Richard E. Douthwaite,† Mark A. Green, Malcolm L. H. Green and Matthew J. Rosseinsky*

Inorganic Chemistry Laboratory, University of Oxford, South Parks Road, Oxford, UK OX1 3QR

The preparation of $[N(CH_3)_4]C_{60}\cdot 1.5thf$ and characterisation of its electronic properties, using susceptibility, EPR and ^{13}C MAS NMR measurements, is reported. X-Ray powder diffraction shows a simple hexagonal stacking sequence of close-packed C_{60} layers, with cations and solvent molecules located in the trigonal-prismatic sites. The electronic properties are consistent with narrow-band metallic behaviour at high temperature. A transition in susceptibility and EPR measurements is seen between 200 and 230 K. A similar synthesis affords a C_{60}^{2-} compound with the same simple hexagonal fulleride packing.

C_{60} is an electronegative molecule. One of the most intensely studied aspects of its chemistry is the preparation of compounds containing C_{60}^{n-} fulleride anions.[1] If the counter ions are electropositive metals from Groups I or II, they are small enough to occupy the interstitial sites in close-packed arrays of the fulleride. The resulting salts then have sufficient C_{60}–C_{60} overlap between the frontier t_{1u} orbitals to allow delocalisation of the electrons, yielding metallic conductivity, and superconductivity in some compounds.[2,3] The A_3C_{60} fullerides have the highest superconducting transition temperatures (T_cs) of any systems except the cuprates. Of particular relevance to the search for high-T_c molecular superconductors is the monotonic increase in T_c with volume per C_{60}^{3-} anion in this series.[4] The highest T_c observed to date is that of 40 K for Cs_3C_{60}, a metastable material produced by low-temperature synthesis.[5] In conventional solid-state synthesis, at the temperatures required to prevent C_{60} decomposition (<650–800 °C), the volatility of most metallic elements is low and cation mobility in the C_{60} lattice can be insufficient for reaction. The use of solution-chemistry routes to new fullerides can circumvent these problems, allowing access to a wide range of structural types and interesting physical properties, and opening up the possibility of extending the number of fullerides with molecular counter ions. On the other hand, cation solvation may prevent fulleride close packing. The known superconductors K_3C_{60} and Rb_3C_{60} have been synthesised from solution,[6–9] as have several novel fulleride salts with organic counter cations such as $[P(C_6H_5)_4]_2C_{60}[I]_{0.35}$,[10] $[P(C_6H_5)_4]_2C_{60}[Cl]$,[11] $\{N[P(C_6H_5)_3]_2\}C_{60}$[12] and $\{N[P(C_6H_5)_3]_2\}_2C_{60}$[13] $\{N[P(C_6H_5)_3]_2{=}PPN\}$ and the ternary fulleride Ba_2CsC_{60}.[14]

The elemental closed-shell counter cations discussed in the preceding paragraph have spherical symmetry and a restricted size range. The electronic properties of the fulleride are controlled by the inter-C_{60} separation and the relative orientations of the C_{60} molecules. Molecular, as opposed to elemental, cations offer a wider distribution of sizes. In addition, the molecular shape can influence the fulleride packing and orientation. A first step in the use of non-elemental cation size and shape to control the electronic properties of fulleride salts was the formation of complex counter cations by ligand coordination to the intercalated metals. Na_2CsC_{60}[15] affords $(NH_3)_4Na_2CsC_{60}$ containing the tetrahedral $(NH_3)_4Na^+$ species on the octahedral site, body-centred tetragonal $(NH_3)K_3C_{60}$ is prepared from K_3C_{60}[16] while face-centred cubic (fcc) Na_3C_{60} yields body-centred cubic (bcc) $(NH_3)_6Na_3C_{60}$[17] with linear $(NH_3)_2Na^+$ groups. Salts of large molecular counter cations do not show fulleride close packing: direct $C_{60}\cdots C_{60}$ contact is lost as both cation and anion take part in the packing to form the solid. The double salts $[P(C_6H_5)_4]_2C_{60}Cl$[11] and $[P(C_6H_5)_4]_2C_{60}I_{0.3}$,[10] and $(PPN)C_{60}$[12] and $(PPN)_2C_{60}$[13] all have crystal structures with large interfulleride separations. $TDAEC_{60}$ [where TDAE is tetrakis(dimethylaminoethylene)] has 10 Å $C_{60}\cdots C_{60}$ contacts in one dimension[18] and is a molecular ferromagnet with $T_c = 16$ K.[20]

In this paper, we report the solution synthesis, reactivity, magnetic and electronic properties of $[N(CH_3)_4]C_{60}\cdot 1.5thf$. Tetraalkylammonium C_{60} compounds have been studied at electrode surfaces[20–22] but no bulk preparations or characterisation have been reported. The route adopted here is amenable to the preparation of molecular fullerides of higher charge, and the preparation and structure of the dianion salt $[N(CH_3)_4]_2C_{60}\cdot xCH_3CN$ is also reported.

Experimental

Materials

Pure C_{60} powder was obtained by spark erosion,[23] chromatography on alumina and sublimation under a dynamic vacuum of 10^{-3} Torr at 500 °C.

$NaC_{60}\cdot 5thf$ was prepared as described previously.[24] $N(CH_3)_4F$ was prepared by a modified literature method.[25] $N(CH_3)_4F\cdot 4H_2O$ (Aldrich) was recrystallised three times from isopropyl alcohol [refluxed and distilled from CaH_2 (twice)] and the resulting alcoholate decomposed at 80 °C under dynamic vacuum (10^{-1} Torr). Purity was checked by ^1H NMR spectroscopy and elemental analysis.

Solvents were distilled under dinitrogen from sodium potassium alloy (thf) and CaH_2 (CH_3CN). CD_3CN was distilled from CaH_2 (twice), degassed using freeze–thaw cycles, and stored under argon.

Synthesis

All samples were manipulated in a helium-filled MBraun Labmaster drybox, where a 25 W light bulb with a 1 cm hole would typically burn for 5 days. Reactions were performed under argon using standard Schlenk techniques with dual argon and vacuum manifolds.

$[N(CH_3)_4]C_{60}\cdot 1.5thf$ was prepared *via* salt metathesis of $NaC_{60}\cdot 5thf$ with $N(CH_3)_4F$ in acetonitrile at −30 °C. $NaC_{60}\cdot 5thf$ is an oxygen- and water-sensitive compound in the solid state and in solution. It is appreciably soluble in thf, CH_3CN and decomposes in EtOH and slowly in CH_2Cl_2. The tetramethylammonium halides (Cl, Br and I) are insoluble in thf and CH_3CN at room temperature but are soluble in solvents such as alcohols and water. $N(CH_3)_4F$ is insoluble in thf, reacts with CH_3CN at room temperature and is soluble in alcohols without decomposition.[25] However, reaction with

CH_3CN is slowed at lower temperatures and is negligible below $-30\,°C$. This allows the metathesis reaction with $NaC_{60}\cdot 5thf$ to be carried out in CH_3CN at low temperature.

At $-30\,°C$ a CH_3CN solution (20 ml) of $N(CH_3)_4F$ (6.4 mg, 0.07 mmol) was added rapidly *via* cannula to a CH_3CN solution (40 ml) of $NaC_{60}\cdot 5thf$ (75.0 mg, 0.07 mmol). The volatiles were removed under reduced pressure at $-30\,°C$ and the black residue extracted with thf (2×20 ml) at room temperature giving an intense cherry red solution and leaving a pale grey residue. The red thf solution was concentrated to *ca.* 2 ml and cooled to $-80\,°C$ depositing black needle-like crystals in the supernatant. Filtration at $-78\,°C$ and washing with pentane (2×5 ml) gave black fern-like microcrystals of $[N(CH_3)_4]C_{60}\cdot 1.5thf$ in 80–90% yield. Filtration at $-78\,°C$ and drying under reduced pressure or under a stream of Ar produced similar results.

The black microcrystalline solid is considerably less oxygen- and moisture-sensitive than $NaC_{60}\cdot 5thf$ and can be handled in air for a few seconds without significant decomposition. It is soluble in CH_3CN and is extremely soluble in thf (>25 mg ml^{-1}), in contrast to $NaC_{60}\cdot 5thf$ which has a considerably reduced solubility in thf and CH_3CN (<5 mg ml^{-1}).

Elemental analysis corresponded to the composition $[N(CH_3)_4]C_{60}\cdot 1.5thf$: found (calc.): C, 91.4 (93.1); H, 2.6 (2.7); N, 1.5 (1.6); Na, <0.1% (0). Integration of the ^1H NMR (CD_3CN) resonances of thf, $N(CH_3)_4^+$ and an internal calibrant of ferrocene of several samples from separate preparations also gave a stoichiometry of $[N(CH_3)_4]C_{60}\cdot(1.5\pm 0.1)thf$. NIR spectroscopy in CH_3CN showed a band at 1080 nm which is in accordance with the C_{60} species in solution being a radical monoanion.[26]

The alkali-metal fullerides Na_2C_{60}, K_3C_{60} and K_4C_{60} are all soluble in CH_3CN and can also be reacted with $N(CH_3)_4F$ at $-30\,°C$ and then extracted at room temperature with CH_3CN (this is necessary as none of these compounds are appreciably soluble in thf) to form $[N(CH_3)_4]_2C_{60}\cdot xCH_3CN$, $[N(CH_3)_4]_3C_{60}\cdot xCH_3CN$ and $[N(CH_3)_4]_4C_{60}\cdot xCH_3CN$, respectively.

Powder X-ray diffraction

Samples were contained in 0.5 mm diameter capillaries sealed under helium. Data was collected in transmission geometry on a Siemens D5000 instrument with a 6 degree linear position-sensitive detector and monochromatic Cu-Kα_1 radiation from a Ge(111) incident beam monochromator.

Solid-state NMR spectroscopy

Samples for ^{13}C magic angle spinning (MAS) NMR spectroscopy (*ca.* 50 mg) were contained in a KEL-F insert within a 7 mm zirconia rotor and spun typically at *ca.* 3 kHz. Samples for static ^{13}C NMR spectroscopy (*ca.* 50 mg) were flame-sealed in 5 mm internal diameter Pyrex tubes. ^{13}C MAS NMR and static spectra were recorded at 50.32 MHz on a Bruker MSL200 spectrometer. Temperature control was achieved using a Bruker VT-1000 temperature control unit. Spectra were referenced externally to adamantane, relative to tetramethylsilane.

Solution NMR spectroscopy

Spectra were recorded on a Bruker AM-300 spectrometer at 300.13 MHz (^1H) referenced internally to the residual protio-solvent resonance of CD_3CN relative to tetramethylsilane.

Magnetic measurements

Dc static susceptibility measurements were performed using a Cryogenic Consultants S600C SQUID magnetometer equipped with a Lakeshore temperature controller. Samples were contained in gelatin capsules with a sample mass of typically 50–80 mg. Correction for the diamagnetism of the container was achieved by measuring the moment of the empty gelatin capsule over a series of temperatures and external fields prior to filling the capsule with sample. Diamagnetic contributions from the core electrons of thf and $N(CH_3)_4^+$ were corrected for using Pascal's constants and those of C_{60} using a correction of -258×10^{-6} emu mol^{-1}.[27]

EPR spectroscopy

Spectra were recorded on a Varian E-LINE Century series X-band spectrometer. Temperature control was achieved using an Oxford Instruments ITC 4 controller. Samples were contained in quartz tubes (Spectrosil) sealed with a Teflon stopcock. Spectra were referenced externally to a powdered sample of α,α'-diphenyl-β-picrylhydrazyl (dpph) radicals and the linewidth taken as peak to peak of the first derivative of the resonance.

Conductivity

The conductivity as a function of temperature from 120 to 300 K was measured using a two-probe dc technique on a section of a pellet ($2\times 5\times 0.5$ mm^3) pressed at room temperature (15 tons) and the four contacts made with silver paint. The sample was mounted on an eight-pin chip and onto a probe on a copper block. The probe was covered with a copper cover, sealed with indium wire and removed from the drybox and placed directly into the cryostat. Temperature control was achieved using an ITC 4 Oxford Instruments intelligent temperature-control unit. Two-probe resistances were measured before and after each experiment in the drybox and confirmed that the sample was not decomposing during the measurement. Measurements were performed on cooling and warming. No significant hysteresis was observed.

Results

Powder X-ray diffraction

The powder X-ray diffraction pattern of $[N(CH_3)_4]C_{60}\cdot 1.5thf$ is shown in Fig. 1. The cell was determined to be hexagonal and refinement of observed reflections gave the cell dimensions as $a=10.131(4)$, $c=10.23(1)$ Å and $V=909.8$ Å^3. These cell parameters correspond to the anions being in van der Waals contact in all three dimensions; the structural motif suggested by the cell size is an AAA stacking of close-packed layers of C_{60} molecules, as previously reported for $(P_4)_2C_{60}$[28,29] and $(I_2)_2C_{60}$.[30] In this simple hexagonal structure, there are only two suitable positions [shown in Fig. 2(*a*)] for species of the size of thf or $N(CH_3)_4^+$ in the unit cell: the two trigonal prismatic sites at ($\pm 1/3$, $\pm 2/3$, 1/2) [these sites are fully

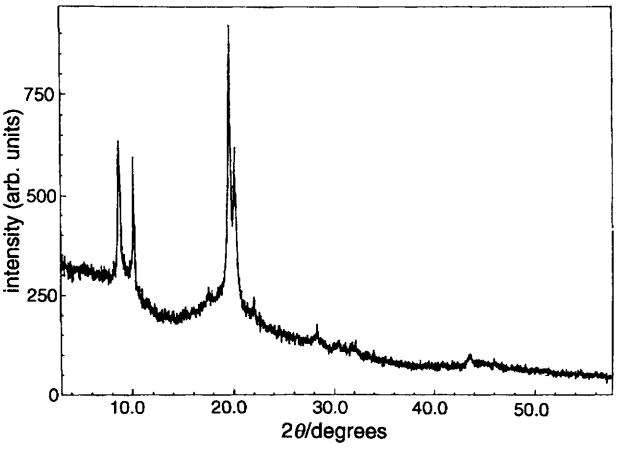

Fig. 1 Powder X-ray diffraction pattern of $[N(CH_3)_4]C_{60}\cdot 1.5thf$

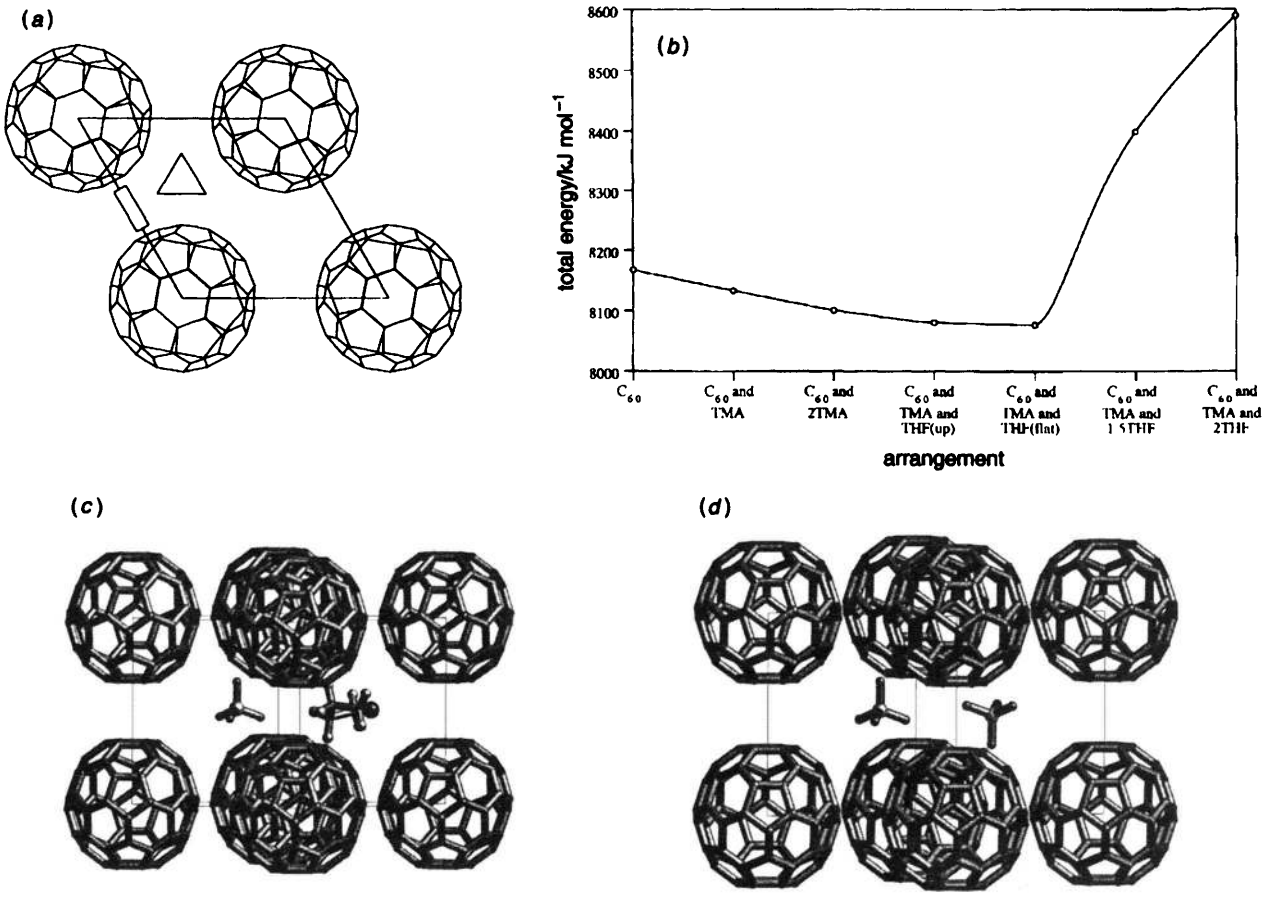

Fig. 2 (*a*) A simple hexagonal array of C_{60} molecules, with the trigonal-prismatic and square-planar sites shown. (*b*) Calculated total energy for various structural arrangements of $[N(CH_3)_4]$ and thf. (*c*) Minimised structure of $[N(CH_3)_4]C_{60}\cdot$thf. (*d*) Minimised structure of $[N(CH_3)_4]_2C_{60}$.

occupied in $(P_4)_2C_{60}]$, or the square sites in the *ac* or *bc* faces at (1/2, 0, 1/2), (0, 1/2, 1/2) or (1/2,1/2,1/2). Molecular mechanics computations, using the consistent-valence forcefield (CVFF) within the BIOSYM software,[31,32] were employed to calculate and minimise the possible locations of the $N(CH_3)_4^+$ and thf molecules. All C_{60} molecules were assumed to be orientationally ordered in the $P\bar{3}$ space group. Introduction of the tetramethylammonium cation into the simple hexagonal array clearly favours the trigonal-prismatic site over the square one. Diffraction patterns were calculated in which these sites are 50% occupied by the tetramethylammonium cation in a positionally disordered manner. However, this model clearly fails to reproduce the observed diffraction pattern [Fig. 3(*a*)] with the first two reflections calculated to be far too intense, suggesting the importance of modelling the scattering from the included solvent molecules which are required by the analytical and NMR data. Docking and energy-minimisation calculations in a simple hexagonal C_{60} array with half of the trigonal-prismatic sites occupied by the tetramethylammonium cations shows the thf molecules also prefer the trigonal-prismatic site over the square one. Two orientations of the thf, one with the molecular plane parallel and the other with this plane perpendicular to the layer stacking direction, are found to have very close total energies. The composition $[N(CH_3)_4]C_{60}\cdot$thf [Fig. 2(*c*)] has a diffraction pattern [Fig. 3(*b*)] which depends only slightly on the orientation of the thf (shown as parallel). It is, therefore, impossible to determine this orientation with the present data. Calculations were then performed to explore the inclusion of a second thf molecule into the structure. It was found that two molecules can occupy the trigonal site, but with a considerable total energy increase over the single occupied arrangement, as shown in Fig. 2(*b*). Minimisation shows that these two molecules are both aligned parallel to the stacking direction, with a substantial energy increase if they are ordered perpendicular. Occupation of the square site is much higher in energy and thus ignored in the subsequent discussion. The possibility of solvent molecules occluded on the surface of the crystals makes the 1.5 thf molecules per formula unit an upper limit. Therefore, it is proposed that the observed composition results from predominantly single occupation of the trigonal sites by thf, with the possibility of a random distribution of doubly occupied sites. The inclusion of 50% extra thf produces a calculated diffraction pattern which is still in reasonable agreement with the observed pattern, shown in Fig. 3(*c*).

$[N(CH_3)_4]_2C_{60}\cdot xCH_3CN$ is also hexagonal and refinement of eight reflections gives cell parameters $a=10.226(2)$, $c=9.978(7)$ Å and $V=903.6$ Å^3. The diffraction pattern can be approximately modelled by full occupancy of the trigonal prismatic sites by the tetramethylammonium cation [Fig. 2(*d*)]. The observed and calculated powder X-ray diffraction patterns of $[N(CH_3)_4]_2C_{60}$ are shown in Fig. 4. Rietveld refinement using the program PROFIL[33] with spherical shell scattering from the C_{60} and the $N(CH_3)_4$ cations gives $R_I=18\%$, suggesting the model requires further modification for satisfactory agreement with the data.

^{13}C solid-state NMR spectroscopy

^{13}C NMR spectroscopy has been used extensively to probe the dynamics and relaxation mechanisms of alkali-metal fullerides and is an integral technique in the determination of the phase purity of a material containing C_{60}. The room-temperature $^{13}C\{^1H\}$ MAS NMR spectrum of $[N(CH_3)_4]C_{60}\cdot 1.5$thf at 50.32 MHz shows only a single peak at δ 185 ($\nu_{1/2}<100$ Hz) (Fig. 5) which is assigned to the C_{60} monoanion. No ^{13}C

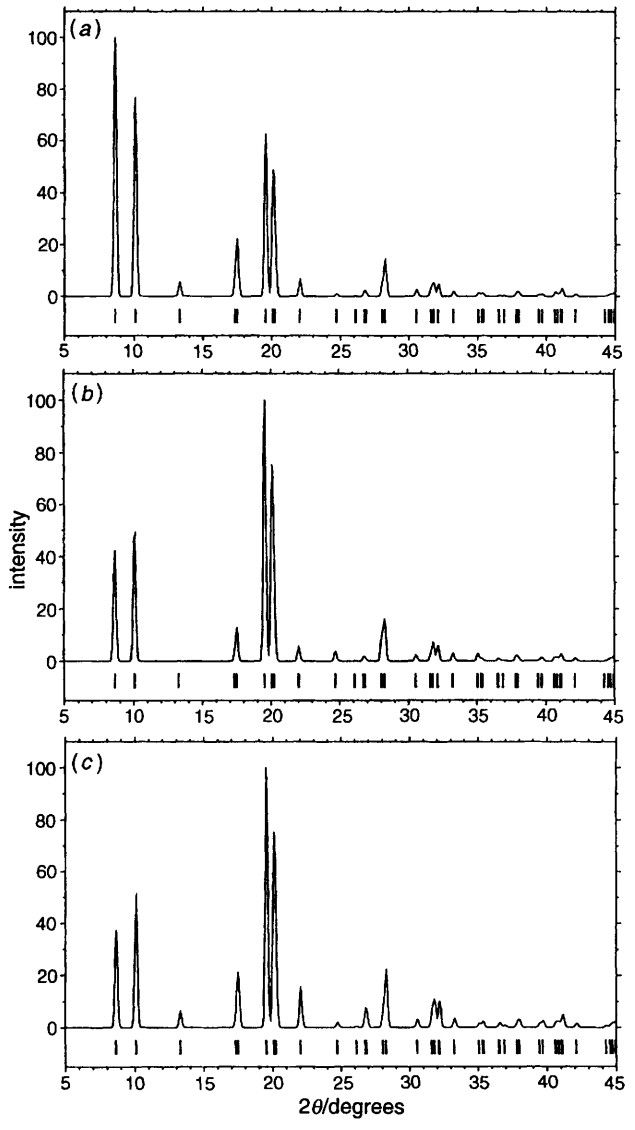

Fig. 3 Powder X-ray diffraction patterns generated using BIOSYM software from the structures in Fig. 2 for: (*a*) $[N(CH_3)_4]C_{60}$; (*b*) $[N(CH_3)_4]C_{60}\cdot thf$; (*c*) $[N(CH_3)_4]C_{60}\cdot 1.5thf$

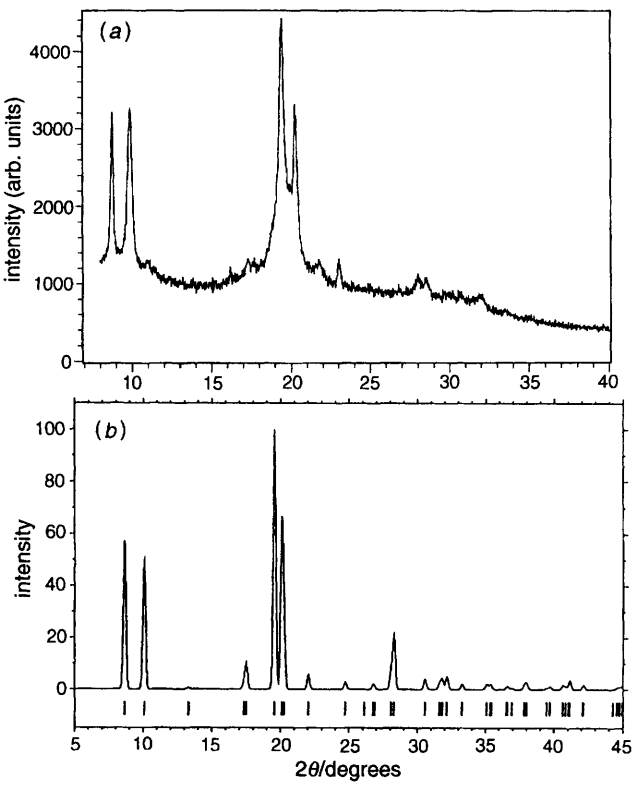

Fig. 4 (*a*) Observed powder X-ray diffraction pattern of $[N(CH_3)_4]_2C_{60}$; (*b*) X-ray powder diffraction pattern calculated according to the model of Fig. 2(*d*)

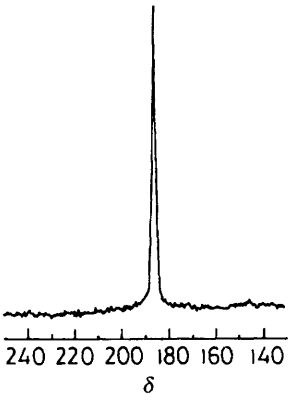

Fig. 5 Room-temperature ^{13}C MAS NMR spectrum of $N(CH_3)_4C_{60}\cdot 1.5thf$

resonances could be observed from the thf or $N(CH_3)_4^+$ moieties (relaxation delays from 0.5 to 60 s were used). $^{13}C\{^1H\}$ CP MAS NMR with contact times ranging from 0.5 to 50 ms did not show any resonances except the single peak at δ 185 ppm. This could be due to positional disorder of thf and $N(CH_3)_4^+$ plus orientational disorder of the fulleride resulting in the occupation of a large number of slightly differing sites and a very broad resonance, or broadening of the resonance by local moments on adjacent fulleride anions. Exposure of the solid to air resulted in decomposition over a period of minutes which was monitored by $^{13}C\{^1H\}$ MAS NMR and showed new peaks at δ 143 and 55 assigned to C_{60} powder and the $N(CH_3)_4^+$ cation, respectively. Peaks corresponding to thf were not observed. This is probably due to evaporation of thf from the decomposing sample. Decomposition is accompanied by a colour change from black to tan brown.

The room-temperature $^{13}C\{^1H\}$ static NMR spectrum of $[N(CH_3)_4]C_{60}\cdot 1.5thf$ at 50.32 MHz showed a single peak at δ 185 ($\nu_{1/2}=500$ Hz) (Fig. 6). This indicates that the C_{60} monoanions are undergoing isotropic reorientation which is fast ($>10^4$ s^{-1}) on the NMR timescale and thus averages out the chemical shift anisotropy. Cooling the sample below 200 K (Fig. 6) results in broadening and a large change in the chemical shift to lower field. The broadening is either due to restriction of the reorientation of the $C_{60}^{\cdot -}$ anions or to enhanced relaxation produced by local magnetic moments. The isotropic chemical shift (defined as the centre of gravity of the resonance) changes abruptly below 200 K, in agreement with the magnetisation and EPR measurements, but its temperature dependence cannot be fitted to a Curie–Weiss law at any temperature. The temperature independence of the shift at 230 K and above is consistent with metallic behaviour in this temperature range. The ^{13}C MAS NMR spectra of the $[N(CH_3)_4]_xC_{60}$ fullerides produced by reaction of $N(CH_3)_4F$ with the C_{60}^{n-} anions are shown in Fig. 7 (*a*)–(*c*). They show a common feature at δ 180, which we assign to $[N(CH_3)_4]_2C_{60}$.

Magnetic measurements

Dc magnetic susceptibility measurements of $[N(CH_3)_4]C_{60}\cdot 1.5thf$ as a function of temperature at 1 T show non-Curie–Weiss behaviour over the entire temperature range and a large drop in the susceptibility at *ca.* 200 K (Fig. 8). The susceptibility as a function of temperature after zero-field cooling

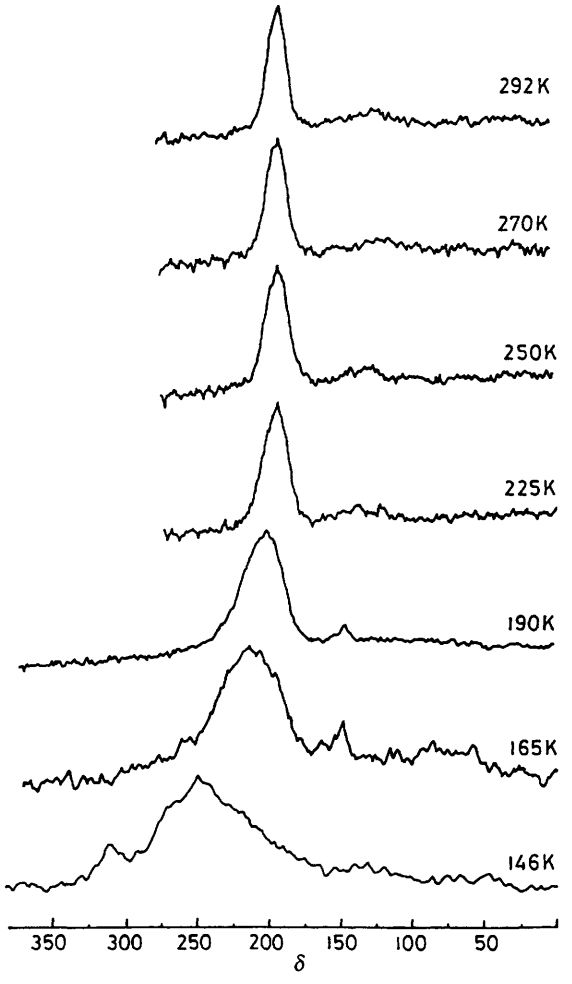

Fig. 6 ^{13}C wideline (static) NMR spectra of $[N(CH_3)_4]C_{60}\cdot 1.5thf$ at the temperatures indicated. Spectra were filled to 4096 points and 50 Hz Lorentzian line broadening applied (100 Hz at 146 K).

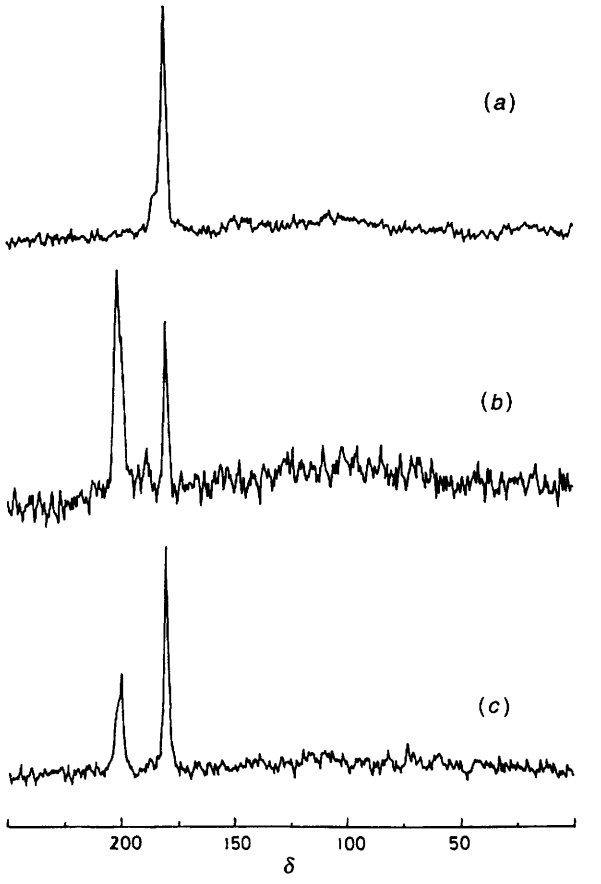

Fig. 7 ^{13}C MAS NMR spectra at room temperature of (*a*) $[N(CH_3)_4]_2C_{60}$; (*b*) the solid product of the reaction of K_3C_{60} and $N(CH_3)_4F$ in CH_3CN; (*c*) K_4C_{60} and $N(CH_3)_4F$ in CH_3CN

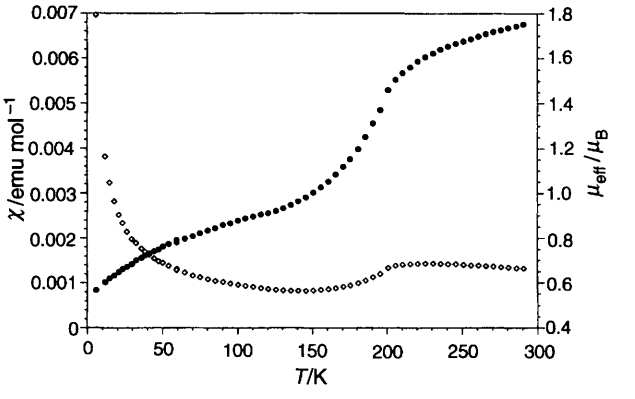

Fig. 8 Dc static susceptibility (open diamonds) measured in a 1 T field and effective magnetic moment (filled circles) as a function of temperature for $[N(CH_3)_4]C_{60}\cdot 1.5thf$

and field (1 T) cooling did not show any hysteresis below or above the transition at 200 K. The magnetisation as a function of applied field at 6 K from 0 to 3 T was linear and did not show hysteresis or saturation.

Attempts to fit the magnetisation data over the whole temperature range were unsuccessful. In itinerant electron systems, sharp drops in magnetisation are observed in the Kondo insulators, which are systems of considerable current interest.[34] FeSi, now considered an early prototype of this class of material, has a qualitatively similar temperature dependent susceptibility to $[N(CH_3)_4]C_{60}\cdot 1.5thf$, but the narrow band equations used to fit its susceptibility fail quantitatively here.[35] As ^{13}C NMR measurements indicate a significant change in the molecular dynamics in the region of the magnetic transition, and the ^{13}C NMR total shift becomes temperature dependent below this transition, we then analysed the data above and below the transition separately. A convenient starting point for understanding the data is to consider the effective magnetic moment per C_{60} $[\mu_{eff}/\mu_B = 2.82(\chi_{mol}T)^{1/2}]$, which is shown in Fig. 8. A localised array of non-interacting $S=1/2$ C_{60}^- anions would have a temperature-independent value of 1.73 μ_B. Although the high-temperature limiting value is indeed 1.7 μ_B, there is no temperature region over which the Curie law is obeyed. At low temperature, below the 200 K transition, fits to $\chi = C/T + A + f(T)$, where $f(T)$ is a slowly varying function of temperature (discussed in more detail with respect to the high-temperature data) and C/T and A represent respectively Curie and temperature-independent contributions to the susceptibility, are successful [Fig. 9(*a*)]. In all the fits, regardless of the precise form of $f(T)$, $C=0.035$–0.04 emu mol^{-1} K, corresponding to a magnetic moment of 0.6 μ_B per C_{60}, and $A=(7\text{–}8)\times 10^{-4}$ emu mol^{-1}.

The data between 230 and 300 K cannot be fitted successfully with the function $\chi = A + C/T$; this functional form has incorrect curvature. The Curie–Weiss law yields a significantly poorer fit than found at low temperature, with unphysically large values of θ (−450 K) and μ_{eff} (2.5 μ_B per C_{60}). The second-order polynomial, $\chi = a + bT + cT^2$, provides a much better fit, with the size of the linear and second-order contributions being comparable to the constant term over this temperature range. This behaviour is appropriate for a metal with a small Fermi energy. Fits to the functional form appropriate to the paramagnon-enhanced correlated metal,[36] $\chi = \chi_{Pauli}[1-(T/AT_F)^2]$ also provide a considerable improvement over the Curie law fits. Including the low-T Curie tail as a

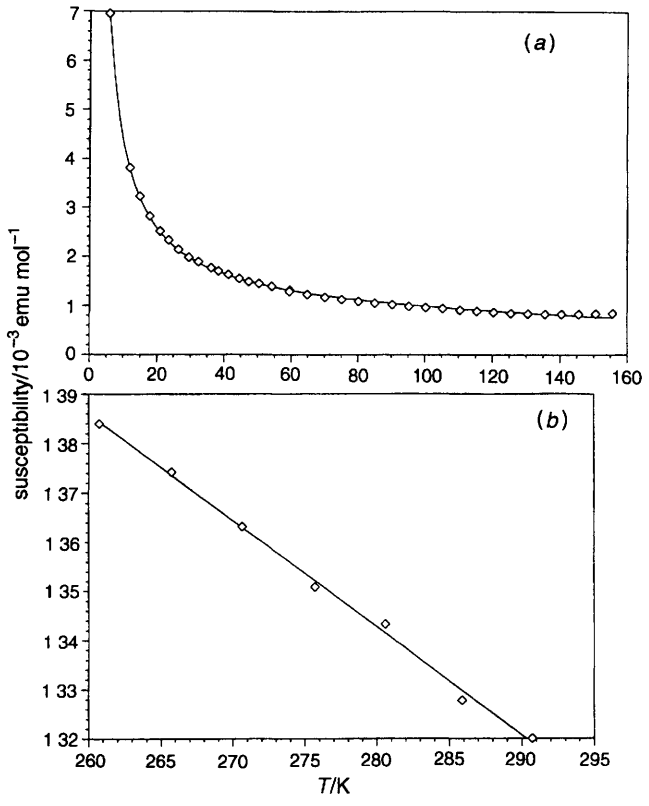

Fig. 9 (*a*) Fit to susceptibility below 160 K as described in the text (*b*) Fit to susceptibility of $[N(CH_3)_4]C_{60}\cdot 1.5thf$ above 260 K as described in the text

fixed term makes little difference to the fit The fit shown in Fig 9(*b*) is to $\chi=\chi_0[1-(T/B)^2]+0.04/T$ with $\chi_0=16\times10^{-4}$ emu mol^{-1} and $B=661$ K

Electron spin susceptibility measurements were performed by double integration of the EPR signal between 130 and 290 K and showed a transition similar to that observed in the dc susceptibility data [Fig 10(*a*)] The linewidth [Fig 10(*b*)]

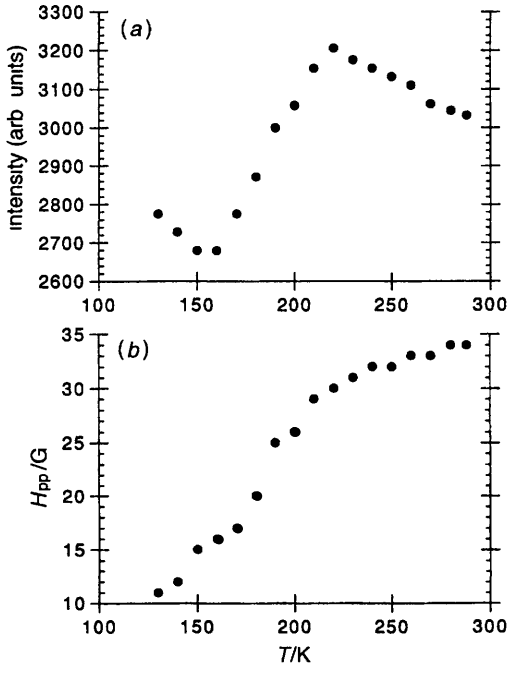

Fig. 10 (*a*) Spin susceptibility of $[N(CH_3)_4]C_{60}\cdot 1.5thf$ derived from integration of EPR spectra as a function of temperature (*b*) EPR peak-to-peak linewidth as a function of temperature for $[N(CH_3)_4]C_{60}\cdot 1.5thf$

above 230 K shows an increase with increasing temperature, as has been noted previously in the literature The *g* value remained constant within experimental error at 2.000 over the temperature range studied A benzonitrile glass of $[N(CH_3)_4]C_{60}\cdot 1.5thf$ did not show any signs of a transition and the linewidth increased with temperature with a constant *g* value of 1.999, consistent with other reports of frozen glass solutions of C_{60}^- [22 24 26]

Conductivity

The room-temperature conductivity of a pressed pellet is 0.01 $\Omega^{-1}cm^{-1}$, and the temperature dependence appears characteristic of a semiconductor with an activation energy of approximately 0.36 eV, a distinct transition is observable below 200 K, which may be associated with the transition seen in the magnetism Significant grain-boundary effects are to be expected in such an unsintered pellet, but the key point for the purposes of the present paper is that the conductivity is significantly higher than in other C_{60}^- salts with isolated fulleride anions

Some reactivity

Exposure of solid $[N(CH_3)_4]C_{60}\cdot 1.5thf$ to air causes oxidation to C_{60}, observed by ^{13}C MAS NMR spectroscopy On exposure to air, a red thf solution of $[N(CH_3)_4]C_{60}\cdot 1.5thf$ deposits a tan-brown solid (C_{60} powder) within 30 s However, a red CH_3CN solution becomes a very deep orange–brown on exposure to air Removal of the volatiles under reduced pressure gives a dark brown–black reflective solid, **1**, which is insoluble in all common organic solvents including CH_3CN ^{13}C MAS NMR spectroscopy of **1** showed a sharp peak at δ 55, assigned to $N(CH_3)_4^+$, and a broad peak centred at δ 143, assigned to a C_{60}-based material (C_{60} itself gives a very sharp resonance at this chemical shift value when pure) Solution ^1H NMR spectroscopy in CD_3CN of the orange–brown solution formed by exposure of $[N(CH_3)_4]C_{60}\cdot 1.5thf$ to air showed one broad peak at δ 2.3 in addition to the residual protio solvent (Fig 11) Powder X-ray diffraction showed that **1** was amorphous The fact that **1** is formed in CH_3CN and not thf strongly suggests that CH_3CN is involved in a reaction with C_{60}^- in the presence of air Compound **1** is then possibly the result of polymerisation/oligomerisation of (or initiated by) C_{60}-based radicals on removal of the volatiles from the orange–brown CH_3CN solution Species **1** does not have an observable EPR spectrum at room temperature and it is essentially diamagnetic as determined by SQUID magnetometry

Reaction of 1 equiv of $[N(CH_3)_4]C_{60}\cdot 1.5thf$ with $[Fe(\eta\text{-}C_5H_5)(CO)_2Cl]$ in thf gave $[Fe(\eta\text{-}C_5H_5)(CO)_2]_2$, C_{60} and

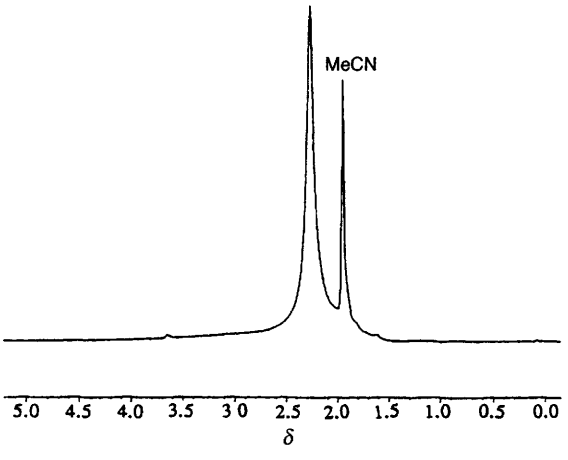

Fig. 11 Solution ^1H NMR spectrum of $[N(CH_3)_4]C_{60}\cdot 1.5thf$ in CD_3CN after exposure to air

$N(CH_3)_4Cl$. This is due to reduction of $[Fe(\eta\text{-}C_5H_5)(CO)_2Cl]$ by $C_{60}^{\cdot -}$.

Suspension overnight of $[N(CH_3)_4]C_{60}\cdot 1.5thf$ with stirring in a solution of 1.5 mol dm^{-3} *n*-butyllithium produced intercalation of lithium cations and presumably reduction of the $[N(CH_3)_4]C_{60}\cdot 1.5thf$ host giving a black solid, **2**. After filtration and washing with hexane, ^7Li MAS NMR spectroscopy showed a broad peak at δ 3 ($\nu_{1/2}=3$ kHz) and ^{13}C MAS NMR studies revealed two peaks at δ 183 and 181 ($\nu_{1/2}\approx 200$ Hz for both). Compound **2** is currently under investigation.

Several attempts at intercalation of rubidium metal at temperatures from 100 to 300 °C caused decomposition of $[N(CH_3)_4]C_{60}\cdot 1.5thf$ as observed by ^{13}C MAS NMR spectroscopy. No superconductivity was observed in these solids, which had broad MAS NMR resonances at δ 145 and 186, tentatively consistent with disproportionation of the monoanion salt into C_{60} and a more reduced fulleride on reaction with rubidium.

Solution ^1H NMR spectroscopy shows that thf can be removed from $[N(CH_3)_4]C_{60}\cdot 1.5thf$ under dynamic vacuum (10^{-3} Torr) at 80 °C, but ^{13}C MAS NMR spectroscopy of the desolvated material always showed a broad peak at δ 143 in addition to a peak at δ 183, indicating that removal of thf is associated with decomposition. Powder X-ray diffraction of the desolvated material showed broad Bragg peaks that precluded confident indexing. $[N(CH_3)_4]C_{60}\cdot 1.5thf$ is prone to loss of crystallinity on prolonged standing in the drybox, which we associate with thf loss.

Discussion

We have isolated simple hexagonal arrays containing close-packed layers of C_{60} anions, with tetramethylammonium as the counter cation. Energy minimisation and powder X-ray diffraction suggest location of the TMA^+ (tetramethylammonium) cations at the trigonal-prismatic sites, although the details of the structures proved inaccessible from the powder data. The lattice parameters show that close packing is still maintained in two dimensions; it is simply the stacking sequence of the layers which changes from ABC to AAA, reducing the number of 10 Å interfulleride contacts from twelve to eight. This is an interesting crystal chemical observation. We may roughly estimate the van der Waals radius of the $N(CH_3)_4^+$ cation as 2.2 Å. The $(NH_3)_4Na^+$ cation is approximately 3.2 Å in size and still occupies the octahedral site in fcc $(NH_3)_4Na_2CsC_{60}$, and therefore an fcc $TMAC_{60}$ with TMA^+ on the octahedral site is not precluded on size grounds. It appears that the absence of small cations suitable to occupy the tetrahedral sites in the fcc structure and the presence of a second large group (the thf solvent or a second tetramethylammonium cation) under the present low-temperature (−30 °C) synthesis conditions favours this simple hexagonal structure. The difference from the denser, close packed structures is that there are two large sites per C_{60} (the trigonal-prismatic ones), rather than the single octahedral site available in fcc structures, and so the presence of two large groups clearly favours simple hexagonal packing. The second moiety [thf or $N(CH_3)_4^+$] is apparently required to stabilise the hexagonal structure, to avoid vacancies on the large trigonal prismatic sites; this is demonstrated by the instability of the $x=1$ material when desolvated.

The C_{60}–C_{60} distances in $(PPN)_xC_{60}$ ($x=1$, 2) and $[P(C_6H_5)_4]_2C_{60}$ (X=Br, I) are considerably greater than 10 Å, accounting for their strongly insulating character. $[N(CH_3)_4]C_{60}\cdot 1.5thf$ is more conducting than these salts and has a transition in its magnetic susceptibility. The absence of any signature of the transition in the frozen-glass EPR spectra indicates that the transition is a solid-state effect, arising from the close interfulleride contacts. No hysteresis is observed and ^{13}C wideline NMR studies do not show any signs of large line broadenings or of extra resonances. It therefore seems unlikely that the transition in $[N(CH_3)_4]C_{60}\cdot 1.5thf$ is due to cycloaddition producing poly- or oligo-merisation/dimerisation, which is found for the A_1C_{60} systems (A=K, Rb, Cs).

Transitions of the sort observed in $[N(CH_3)_4]C_{60}\cdot 1.5thf$ have been found in the compounds $Na_xC_{60}.ythf$ (where $x=0.36$–0.42 and $y=1.5$–2.9),[37] $NaC_{60}\cdot 3thf$ [38] and $NaC_{60}\cdot 5thf$.[24] In the case of $Na_xC_{60}\cdot ythf$ (where $x=0.36$–0.42 and $y=1.5$–2.9) a metal–metal transition occurs at 180 K, with an increase in single-crystal conductivity from a virtually temperature-independent value of 50 S cm^{-1} to a maximum value of *ca.* 1000 S cm^{-1} at 100 K.

The observation of broadening of the ^{13}C NMR spectra without hysteresis suggests that the transition in $[N(CH_3)_4]C_{60}\cdot 1.5thf$ is closely associated with a slowing down of the reorientation dynamics of the C_{60}^- species. Given the close interfulleride contacts in the simple hexagonal structure, any structural transition will strongly influence the physical properties by changing the nearest-neighbour transfer integral.

The localised electron analysis of χ above 230 K produces unphysical parameters. An itinerant electron analysis is consistent with the high powder conductivity compared with $(PPN)_xC_{60}$ and $[P(C_6H_5)_4]_2C_{60}Cl$. The temperature-independent terms in the fit above 230 K are close to χ_{Pauli} found for many fulleride metals [$\chi(K_3C_{60})=10\times 10^{-4}$ emu mol^{-1}]. The tight-binding bandwidth, $W=2zt$, may be estimated as 0.4 eV, using $z=8$ and $t=0.025$ eV (from K_3C_{60}).[39] This is compared with estimates of the Hubbard U of 1–1.5 eV,[40] suggesting that it is appropriate to use the paramagnon model for spin fluctuations produced by interelectron repulsion in narrow-band metals to analyse the data. Here, the density of states at the Fermi energy, E_F, evaluated from the magnetic response, N_χ, ($\chi=2\mu_B^2N_\chi$, where N_χ is per spin, *i.e.* orbital states) is enhanced over that predicted from the bare density of states, N_B, as $N_\chi=N_B/(1-IN_B)$ where I is the Stoner parameter. In addition, excitation of paramagnons due to the incipient local moment character (spin fluctuations) gives the susceptibility a temperature dependence in narrow band systems. A quantitative expression for this is $\chi=\chi_{Pauli}[1-3.2\pi^2/24K^2(T/T_F)^2]$, where $K=1-IN_B$ [see the fit in Fig. 9(*b*)]. Here $\chi=16\times 10^{-4}$ emu mol^{-1} yields $N_\chi=20$ states eV^{-1} $spin^{-1}$ C_{60}^{-1}. We then use a free-electron estimate of N_B of 8 states eV^{-1} C_{60}^{-1} $spin^{-1}$ to find a Stoner enhancement of the susceptibility of the order of 2.5 (similar to that found for K_3C_{60}[41]) and an unenhanced Fermi temperature of 1865 K. The free-electron Fermi temperature with one electron per C_{60} in a triply degenerate band is 1800 K and so the magnitude and temperature dependence of the susceptibility are consistent with the correlated itinerant electron model.

Within this interpretation of the high temperature data, the transition at 230 K would be due to significant changes in the transfer integrals being associated with the change in molecular dynamics indicated by the variable-temperature NMR measurements. The transition would then be similar to the metal–metal transition seen in $Na_xC_{60}\cdot ythf$ ($x=0.36$–0.42, $y=1.5$–2.9). However, in order to account for the substantial Curie tail at low temperature, either 10% $S=1/2$ impurities (extraneous or trapped at C_{60} sites in the otherwise metallic solid) must be present in the sample, or the electronic structure of the solid is such that each C_{60} carries a local moment of 0.6 μ_B in the metallic state. An alternative interpretation of the transition is therefore as a metal–insulator transition where the delocalised electrons become 0.6 μ_B local moments on the C_{60} anions and the constant term A, derived from the analysis of the low-temperature data, is ascribed to van Vleck temperature-independent paramagnetism. This description of the low-temperature state is consistent with either localised or delocalised models for the high-temperature behaviour and would agree with the temperature dependence of the ^{13}C shift below

the transition The small local moment can then be ascribed to use of the simple Curie model in a situation where assignment of electronic character as purely localised is oversimplified

The small variation of the EPR linewidth with temperature at high temperature is also suggestive of metallic behaviour above the transition Quantitative interpretation of the linewidth may be made following Janossy *et al*[42] and results in a conduction electron scattering time of $\tau_R = 4 \times 10^{-14}$ s, four times smaller than that found for Rb_3C_{60} The physically sensible values derived from analysis of the high-temperature phase EPR and χ data with the assumption of a narrow-band metal increase our confidence in this assignment Below 200 K, the temperature dependence of the linewidth is more marked, suggestive of either a longer, more temperature-dependent τ_R in the more highly conducting metallic phase, or a transition to a localised C_{60}^- system

$[N(CH_3)_4]C_{60} \cdot 1.5thf$ is an example of a C_{60} monoanion salt in which the single t_{1u} electron does not promote the formation of oligomeric or polymeric units, despite the close interfulleride contacts The magnetic data show that strong interactions between the t_{1u} electrons make the magnetic response considerably more complex than would be expected from a localised array of C_{60}^- anions a coherent interpretation of the EPR, susceptibility and conductivity data is possible within an itinerant electron model above the transition, but a decisive distinction between strongly coupled local spins and a narrow-band metal is difficult without further measurements, preferably on single crystals, which will help resolve the precise nature of the transition at 230 K The structural chemistry provides a contrast with that of the larger alkali-metal cations and the fullerides of complex ammoniated cations in that the close-packed fulleride layers are stacked in a simple hexagonal AAA manner, this seems to require the presence of two large guest species (cation or solvent molecule), which occupy the two trigonal-prismatic sites in this array

We thank Dr Mohammed Kurmoo of the Royal Institution for assistance with the conductivity measurement, St John's College, Oxford for a Junior Research Fellowship to R E D and the EPSRC for a grant towards the purchase of the powder diffractometer

References

1 D W Murphy, M J Rosseinsky, R M Fleming, R Tycko, A P Ramirez, R C Haddon, T Siegrist, G Dabbagh, J C Tully and R E Walstedt, *J Phys Chem Solids*, 1992, **53**, 1321
2 A F Hebard, M J Rosseinsky, R C Haddon, D W Murphy, S H Glarum, T T M Palstra, A P Ramirez and A R Kortan, *Nature (London)*, 1991, **350**, 600
3 R C Haddon, A F Hebard, M J Rosseinsky, D W Murphy, S J Duclos, K B Lyons, B Miller, J M Rosamilia, R M Fleming, A R Kortan, S H Glarum, A V Makhija, A J Muller, R H Eick, S M Zahurak, R Tycko, G Dabbagh and F A Thiel, *Nature (London)*, 1991, **350**, 320
4 R M Fleming, M J Rosseinsky, A P Ramirez, D W Murphy, J C Tully, R C Haddon, T Siegrist, R Tycko, S H Glarum, P Marsh, G Dabbagh, S M Zahurak, A V Makhija and C Hampton, *Nature (London)*, 1991, **352**, 701
5 T T M Palstra, O Zhou, Y Iwasa, P E Sulewski, R M Fleming and B R Zegarski, *Solid State Commun*, 1994, **92**, 71
6 R P Ziebarth, D R Buffinger, V A Stenger, C Recchia and C H Pennington, *J Am Chem Soc*, 1993, **115**, 9267
7 H H Wang, A M Kini, B M Savall, K D Carlson, J M Williams, M W Lathrop, K R Lykke, D H Parker, P Wurz, M J Pellin, D M Gruen, U Welp, W-K Kwok, S Fleshler, G W Crabtree, J E Schirber and D L Overmeyer, *Inorg Chem*, 1991, **30**, 2962
8 H H Wang, A M Kini, B M Savall, K D Carlson, J M Williams, K R Lykke, D H Parker, P Wurz, M J Pellin, D M Gruen, U Welp, W-K Kwok, S Fleshler and G W Crabtree, *Inorg Chem*, 1991, **30**, 2838
9 X Liu, W C Wan, S M Owens and W E Broderick, *J Am Chem Soc*, 1994, **116**, 5489
10 A Penicaud, A Perez-Benitez, R Gleason, E Munoz and R Escudero, *J Am Chem Soc*, 1993, **115**, 10392
11 U Bilow and M Jansen, *J Chem Soc Chem Commun*, 1994, 403
12 H Kobayashi, H Moriyama, A Kobayashi and T Watanabe, *J Am Chem Soc*, 1993, **115**, 1185
13 P Paul, Z Xie, R Bau, P P W Boyd and C A Reed, *J Am Chem Soc*, 1994, **116**, 4145
14 A C Duggan, J M Fox, S J Heyes, P F Henry, D Laurie and M J Rosseinsky, *Chem Commun*, 1996, 1191
15 O Zhou, R M Fleming, D W Murphy, M J Rosseinsky, A P Ramirez, R B van Dover and R C Haddon, *Nature (London)*, 1993, **362**, 433
16 M J Rosseinsky, D W Murphy, R M Fleming and O Zhou, *Nature (London)*, 1993, **362**, 433
17 P F Henry, M J Rosseinsky and C J Watt, *J Chem Soc Chem Commun*, 1995, 2131
18 P W Stephens, D Cox, J W Lauher, L Mihaly, J B Wiley, P-M Allemand, A Hirsch, K Holczer, Q Li, J D Thompson and F Wudl, *Nature (London)*, 1992, **355**, 331
19 P-M Allemand, K C Khemani, A Koch, F Wudl, K Holczer, S Donovan, G Gruner and J D Thompson, *Science*, 1991, **253**, 301
20 R G Compton, R A Spackman, R G Wellington, M L H Green and J Turner, *J Electroanal Chem*, 1992, **327**, 337
21 R G Compton, R A Spackman, D J Riley, R G Wellington, J C Eklund, A C Fischer, M L H Green, R E Douthwaite, A H H Stephens and J F C Turner, *J Electroanal Chem*, 1993, **344**, 235
22 K M Kadish, D Dubois and M T Jones, *J Am Chem Soc*, 1992, **114**, 6446
23 W Kratschmer, L D Lamb, K Fostiropoulos and D R Huffman, *Nature (London)*, 1990, **347**, 354
24 R E Douthwaite, A R Brough and M L H Green, *J Chem Soc Chem Commun*, 1994, 267
25 K O Christie, W W Wilson, R D Wilson, R Bau and J-A Feng, *J Am Chem Soc*, 1990, **112**, 7619
26 C A Reed, J Stinchcombe, A Penicaud, P Bhyrappa and P D W Boyd, *J Am Chem Soc*, 1993, **115**, 5212
27 R C Haddon, L F Schneemeyer, J V Waszczak, S H Glarum, R Tycko, G Dabbagh, A R Kortan, A J Muller, A M Mujsce, M J Rosseinsky, S M Zahurak, A V Makhija, F A Thiel, K Raghavachari, E Cockayne and V Elser, *Nature (London)*, 1991, **350**, 46
28 R E Douthwaite, M L H Green, S J Heyes, M J Rosseinsky and J F C Turner, *J Chem Soc Chem Commun*, 1994, 1367
29 I W Locke, A D Darwish, H W Kroto, K Prassides, R Taylor and D R M Walton, *Chem Phys Lett*, 1994, **225**, 186
30 Q Zhu, D E Cox, J E Fischer, K Kniaz, A R McGhie and O Zhou, *Nature (London)*, 1992, **355**, 712
31 P Dauber-Osguthorpe, V A Roberts, D J Osguthorpe, J Wolff, M Genest and A T Hagler, *Proteins Structure Function and Genetics*, 1988, **4**, 31
32 *InsightII User Guide*, Biosym/MSI, 1995
33 J K Cockcroft, PROFIL Rietveld refinement program, 1991
34 G Aeppli and Z Fisk, *Comments Condens Mater Phys*, 1992, **16**, 155
35 V Jaccarino, G K Wertheim, J H Wernick, L R Walker and S Arajs, *Phys Rev*, 1967, **160**, 476
36 N F Mott, *Metal–Insulator Transitions*, Taylor and Francis, 1990
37 H Kobayashi, H Tomita, H Moriyama, A Kobayashi and T Wanatabe, *J Am Chem Soc*, 1994, **116**, 3153
38 R E Douthwaite, M A Green, M L H Green and M J Rosseinsky, unpublished results
39 S Satpathy, V P Antropov, O K Anderson, O Jepsen, O Gunnarsson and A I Leichtenstein, *Phys Rev B*, 1992, **46**, 1773
40 R W Lof, M A van Veenendaal, B Koopmans, H T Jonkman and G A Sawatzky, *Phys Rev Lett*, 1992, **68**, 3924
41 A P Ramirez, M J Rosseinsky, D W Murphy and R C Haddon, *Phys Rev Lett*, 1992, **69**, 1687
42 A Janossy, O Chauvet, S Pekker, J R Cooper and L Forro, *Phys Rev Lett*, 1993, **71**, 1091

Paper 6/05952J, *Received 28th August*, 1996